Ceramics-Silikáty 67 (1), 81-86 (2023)
www.ceramics-silikaty.cz doi: 10.13168/cs.2023.0005

CHARACTERISATION AND IN VITRO BIOACTIVITY OF HYDROXYAPATITE EXTRACTED FROM CARP FISH BONES FOR BIOMEDICAL APPLICATIONS

DOAA ABBOOD CHALLOOB*, ALI TAHA SALEH*, #AMMAR Z. ALSHEMARY**, ***, YASSER MUHAMMED****, ISMAIL SECKIN CARDAKLI*****

*Department of Chemistry, College of Science, University of Misan, Misan, Iraq
**Department of Chemistry, College of Science and Technology, Wenzhou-Kean University, Wenzhou, 325060, China
***Biomedical Engineering Department, Al-Mustaqbal University College, Hillah, Babil 51001, Iraq
****Aeronautical Techniques Engineering, AL-Farahidi University, Baghdad, Iraq
*****Department of Metallurgical and Materials Engineering, Atatürk University, Erzurum, 25240, Turkey

#E-mail: aalshema@kean.edu

Submitted January 4, 2023; accepted February 2, 2023

Keywords: Carp fish, Biological hydroxyapatite, Characterisations, Bioactivity

Due to low production costs and safety concerns, fish bones are the most common alternative source of Hydroxyapatite (HA). Furthermore, fish processing companies pollute the environment because they throw away a great deal of fish waste. This study successfully extracted biological HA from the fish bones of common carp (Cyprinus carpio). The bones were washed and boiled in hot water before being calcined for two hours at 200 °C, 400 °C, 600 °C, 800 °C, 900 °C, and 1000 °C. The extracted powders were studied using X-ray diffraction (XRD), Fourier transform infrared (FTIR) spectroscopy, and Field emission scanning electron microscopy (FESEM). The results showed that the HA phase forms crystals when the fish bones are heated to 900 °C. The crystallinity and crystallite size increased significantly as the heating treatment increased. The main functional hydroxyl and phosphate groups are found in the HA structure. The shape of the extracted HA particles was globular. The in vitro dissolution and bioactivity of the biological HA were evaluated using simulated body fluid (SBF) for 1, 3, 7, and 14 days at 37 °C. After the first day in the SBF, the rate of degradation was at its highest, which then gradually decreased. The thickness of the apatite layer significantly increased with a prolonged incubation period. There is hope that biological HA may be useful in the biomedical field.

INTRODUCTION

Clinicians still face difficulties repairing a bone defect caused by persistent illness or trauma. Bone defects larger than a certain size often necessitate using synthetic biomaterials for the repair. It is necessary to employ synthetic biomaterials or a xenograft, a bone segment from a different animal species, due to the scarcity of autologous bone and the risk of infection associated with an allograft. The use of xenogeneic bone material has the advantage of being comparable to the human bone in structure and form [1]. Hydroxyapatite (HA, $Ca_{10}(PO_4)_6OH_2$) is a calcium and phosphate bioceramic. Due to its non-immunogenicity, non-inflammatory nature, and lack of harmful effects, HA has been employed as an artificial bone material [2]. As it has a similar chemical structure to human bones and teeth, the inorganic substance of HA has attracted the interest of experts all around the globe for its potential application in implant surgery [3]. HA powder made via synthetic methods need extra chemicals to strengthen its mechanical strength. Many chemicals are involved in stabilising the structures and fixing them in the human body, which is an issue. The upfront costs and complexity of this approach make it unattractive to mass produce HA. Biological HA can be obtained from natural waste, such as bovine bones [4], fish bones [5], fish scales [6], chicken beaks [3], and chicken bones [7]. In addition, natural HA is less expensive and more straightforward than synthetic methods. Also, using synthetic methods, it is time-consuming and difficult to ensure the consistent quality of the HA product sample [8].

Fish, which are subsequently employed as a raw material in the HA extraction process, are said to have been the source of HA in several different documented reports. Mustafa et al. extracted a pure HA phase with a Ca/P ratio that closely approximates the theoretical HA stoichiometry ratio from tilapia (*Oreochromis niloticus*) fish bones heat treated at 900 °C [8]. Boutinguiza et al. successfully extracted biphasic calcium phosphate from swordfish (*Xiphias gladius*) and Atlantic bluefin

tuna (*Thunnus thynnus*) fish bones heat-treated at 900 °C [9]. Yamamura et al. showed that HA produced from whitemouth croacker (*Micropogonias furnieri*) fish waste calcined at 800 °C has a lot of promise as a biomaterial due to its cheap cost, ease of production, and high biocompatibility [10].

However, there are still information gaps, and fewer discoveries have been made concerning them than from other biological sources. This study aims to extract HA from the unexplored biowaste of carp fish bones. The powder was characterised through X-ray diffraction, Fourier transform infrared spectroscopy, and scanning electron microscopy. Also, the *in vitro* dissolution and a bioactivity analysis were performed using simulated body fluid (SBF) for 14 days at 37 °C.

EXPERIMENTAL

The common carp (*Cyprinus carpio*) were purchased from the local market in Misan-Iraq. The bones were cut up using a sharp knife and placed together once they had been collected. The pieces were cooked for about 4 h in a sealed container to remove any big impurities that had adhered to them. The samples were washed several times with distilled water before being submerged in a 3:1 mixture of acetone and ether for three hours to remove any unseen fat, and were finally dried in a hot air oven at 120 °C for 17 h to prevent the development of shoots during the grinding process. The raw powder was then put through the calcination process, which consisted of it being heated in a furnace at temperatures ranging from 200 to 1000 °C at a rate of 5 °C per minute for a total of 2 h. The results show that the fish bones treated at temperatures ranging from 200 °C to 800 °C have a black or light grey colour (Figure 1). This indicates that the material is amorphous and highly carbonated by the residue of the organic materials. The colour of the fish bone powders changes from light grey to pure milky white when heated between 900 °C and 1000 °C (Figure 1). This demonstrates that the organic materials have been removed, and pure HA particles are crystallised. As a direct result of this, it was shown that the ideal temperature range for forming the HA phase was between 900 °C and 1000 °C.

Using different methods, the white powder was studied to find its microstructure. The phase purity, lattice parameters, crystallite size, and degree of crystallinity were investigated using X-ray diffraction (XRD, Philips1730, Panalytical B.V.). The functional groups, such as hydroxyl, carbonate, and phosphate groups that existed in the obtained powders were investigated using Fourier-transform infrared spectroscopy (FTIR, Nicolet iS50 spectrometer). Field emission scanning electron microscopy (FESEM, Oxford Instruments Swift ED 3000) was used to determine the particle size and shape. A thin layer of gold was applied to the samples beforehand to reduce any produced sparks. ImageJ software was used to determine the average particle size and dispersion by measuring the dimensions of 25 particles selected randomly from the FESEM images.

A model of the simulated body fluid (SBF) was used to assess the degradation and bioactivity of the extracted HA. The specimens, which were in the shape of discs, were put inside polyethylene vials that contained 50 mL of SBF, and then the vials were covered with a lid. They were shaken in a water bath for 1, 3, 7, and 14 days while incubating at 37 °C. At each interval, the discs were meticulously removed from the SBF, rinsed in ethanol and distilled water, and then air-dried at room temperature. The next phase consisted of conducting an FESEM-EDX examination in order to investigate the shape and composition of the apatite layer that had formed on the surface. A small amount of each supernatant was collected at each time point, and the amount of Ca^{2+} ions released was measured using Flame atomic absorption spectroscopy (Al 1200, Aurora, UK).

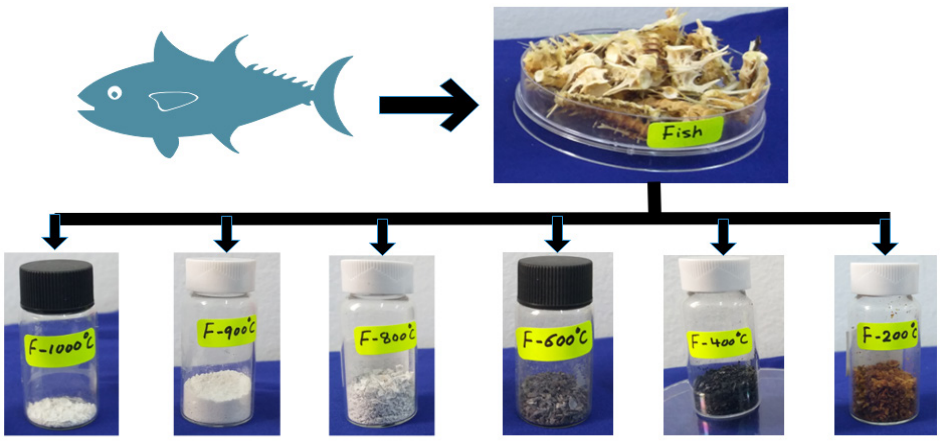

Figure 1. Shows the collected bones treated at different temperatures.

RESULTS AND DISCUSSION

A phase investigation of the HA was carried out with the assistance of XRD (Figure 2). The crystallisation of HA occurs successfully after calcination at temperatures between 900 °C and 1000 °C. The peaks in the XRD pattern for the HA were found to be located at the coordinates (26.12°), (28.45°), (31.15°), (33.20°), (34.28°), (40.11°), (46°), (49.47°), and (55°), and it was determined that these peaks correspond to the (002), (210), (211), (300), (202), (310), (222), (213), and (304) planes of the crystalline HA, respectively. The hexagonal structure of HA has been determined to have the following lattice parameters: a = b = 9.416, c = 6.863, and cell volume = 527.3. The diffraction peaks and lattice parameters were in good agreement with the standard phase of HA (JCDPS No. 09-432). With an increase in the calcination degree to 1000 °C, a tiny peak at 30.71° was observed, which could be attributed to the (0210) diffraction plane of β-tricalcium phosphate (β-TCP, JCDPS No. 09-0169). As a result of the HA decomposition at high temperatures, the β-TCP phase appears as a minor phase [11]. Also, Table 1 shows that there were no big changes in the lattice parameters, the degree of crystallinity, or the size of the crystallites.

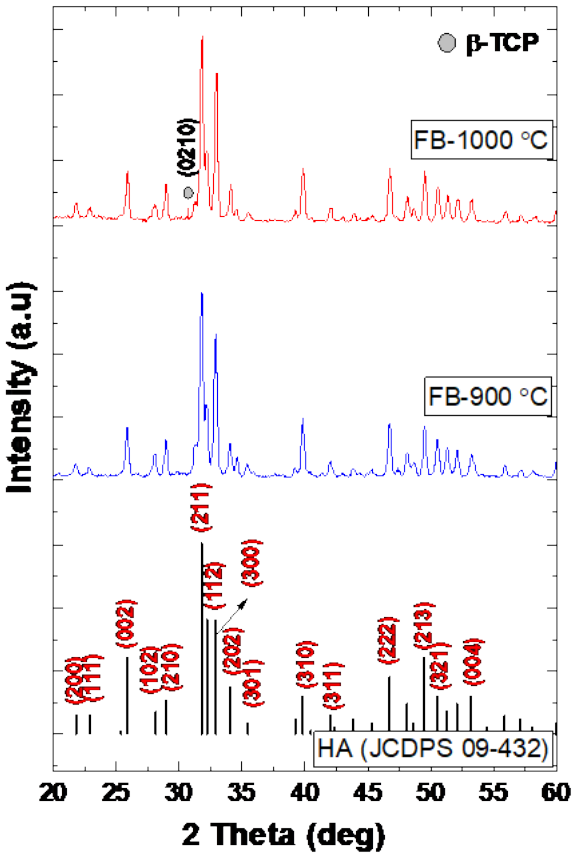

Figure 2. XRD pattern of the fish bones calcined at 900 °C and 1000 °C for 2.

Table 1. Lattice parameters, degree of crystallinity and crystallite size of the biological HA at 900 °C and 1000 °C.

Sample ID	Lattice Parameters			X_c (%)	*CS* (nm)
	a (Å)	*c* (Å)	*V* (Å)^3		
Standard HA	9.418	6.884	528.8	-	-
FB-900 °C	9.416	6.863	527.3	87.77	30.04
FB-1000 °C	9.417	6.860	527.1	79.31	53.79

*Xc = degree of crystallinity; CS = crystallite size

The presence of the functional groups in the extracted HA was detected using an FTIR analysis, and the results are shown in Figure 3. Four vibrational modes of the phosphate (PO_4^{3-}) group were recorded at 466 cm^{-1} (PO_4^{3-} (v4), 565 cm^{-1} (PO_4^{3-} (v2), 604 cm^{-1} (PO_4^{3-} (v2), and 921 – 1200 cm^{-1} (PO_4^{3-} (v1,3). The stretching and bending mode of the hydroxyl (OH)group were observed at 3566 cm^{-1} and 634 cm^{-1}, respectively. Furthermore, the vibrational modes of carbonate (CO_3^{2}) were detected at 1406 cm^{-1} and 1514 cm^{-1}. The presence of carbonate groups indicates the formation of carbonated HA. Nonetheless, the presence of CO_3^{2-} may enhance the bioactivity of HA, so it should not be viewed negatively [12]. The phosphate and hydroxyl bands' sharpness showed crystalline HA formation. Increasing the calcination temperatures to 1000 °C increased the sharpness of the PO_4^{3-} (v1,3) group, which could be attributed to a higher degree of crystallinity (Table 1). While the intensity of the stretching mode of the OH group decreased with an increasing calcination degree, this behaviour could be attributed to HA decomposition to β-TCP.

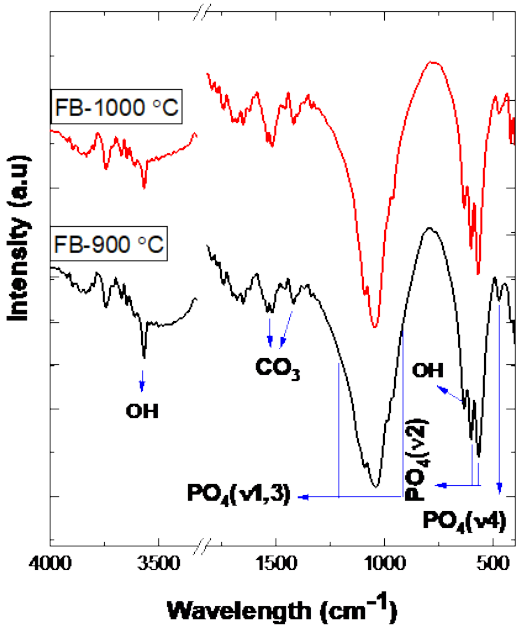

Figure 3. FTIR spectra of the fish bones FB – 900 °C and FB – 1000 °C materials.

The FESEM micrographs of the calcined and extracted powders at 900 °C and 1000 °C showed the particles to be irregularly formed agglomerates that were densely packed together (Figure 4). During the creation of HA particles, one or more of the following steps may occur: (a) the production of HA via nucleation and growth surface-free energy is reduced as a consequence of (b) the aggregation of elemental crystals via the molecular attractions of unique scale forces. This causes a decrease in the surface-free energy. The production of additional crystals inside the aggregates, which occurs under continuous residual supersaturation, leads to the aggregation. After that, the agglomerated particles join forces with other particles to form secondary particles, which subsequently increase in size [12]. There were no significant changes in the morphology of the particles when the calcination temperature was increased to 1000 °C, but the particle size increased significantly.

Table 2. Release of Ca^{2+} ions in the SBF over 14 days at 37 °C.

Immersion time (day)	Release of Ca^{2+} ion ($mg \cdot L^{-1}$) in SBF	
	FB-900 °C	FB-1000 °C
0.0	13.12	12.90
1	23.87	22.88
3	14.79	15.10
7	11.55	10.13
14	9.95	10.07

*STDEV ± 0.32-0.72

that the release of Ca^{2+} ions occurred quite fast, which signalled the beginning of the pellet's dissolution on its most superficial layers. The Ca^{2+} ion concentrations reached their zenith after 24 h of immersion in the SBF, when they were at their maximum. During the first 24 h after the SBF immersion, the deposition process, on the other hand, emerged as the most important step. The consumption of Ca^{2+} ions may explain the drop

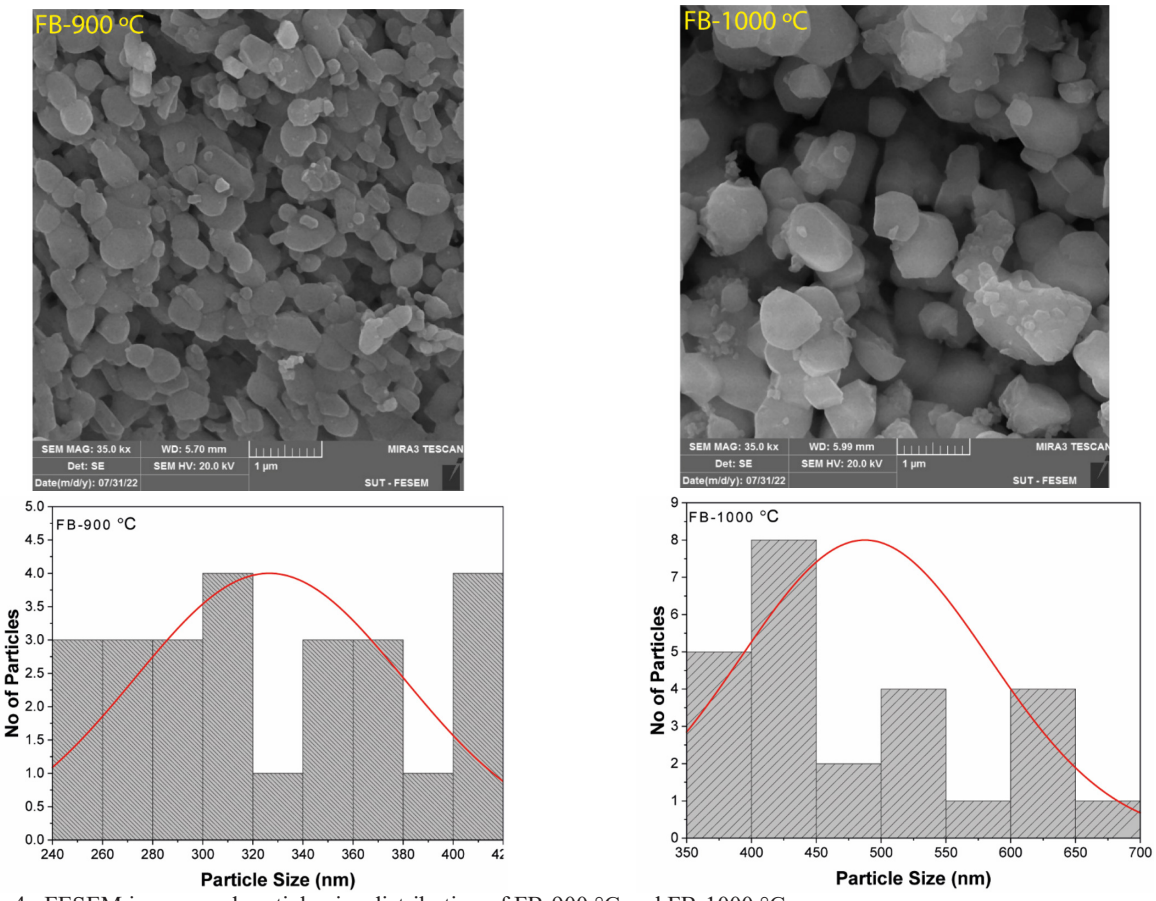

Figure 4. FESEM images and particle-size distribution of FB-900 °C and FB-1000 °C.

The results of the *in vitro* dissolution evaluation using SBF that lasted for 14 days was conducted to determine the dissolution behaviour of FB-900 °C are shown in Table 2. The results provide insight into the possible Ca^{2+} ion concentration present in the SBF throughout the course of a period of 14 days. This table demonstrates in the concentration of Ca^{2+} ions observed during the development of the apatite layer. Maintaining a constant Ca^{2+} concentration level over a period of 7 – 14 days is evidence that a balance has been struck between the processes of deposition and dissolution.

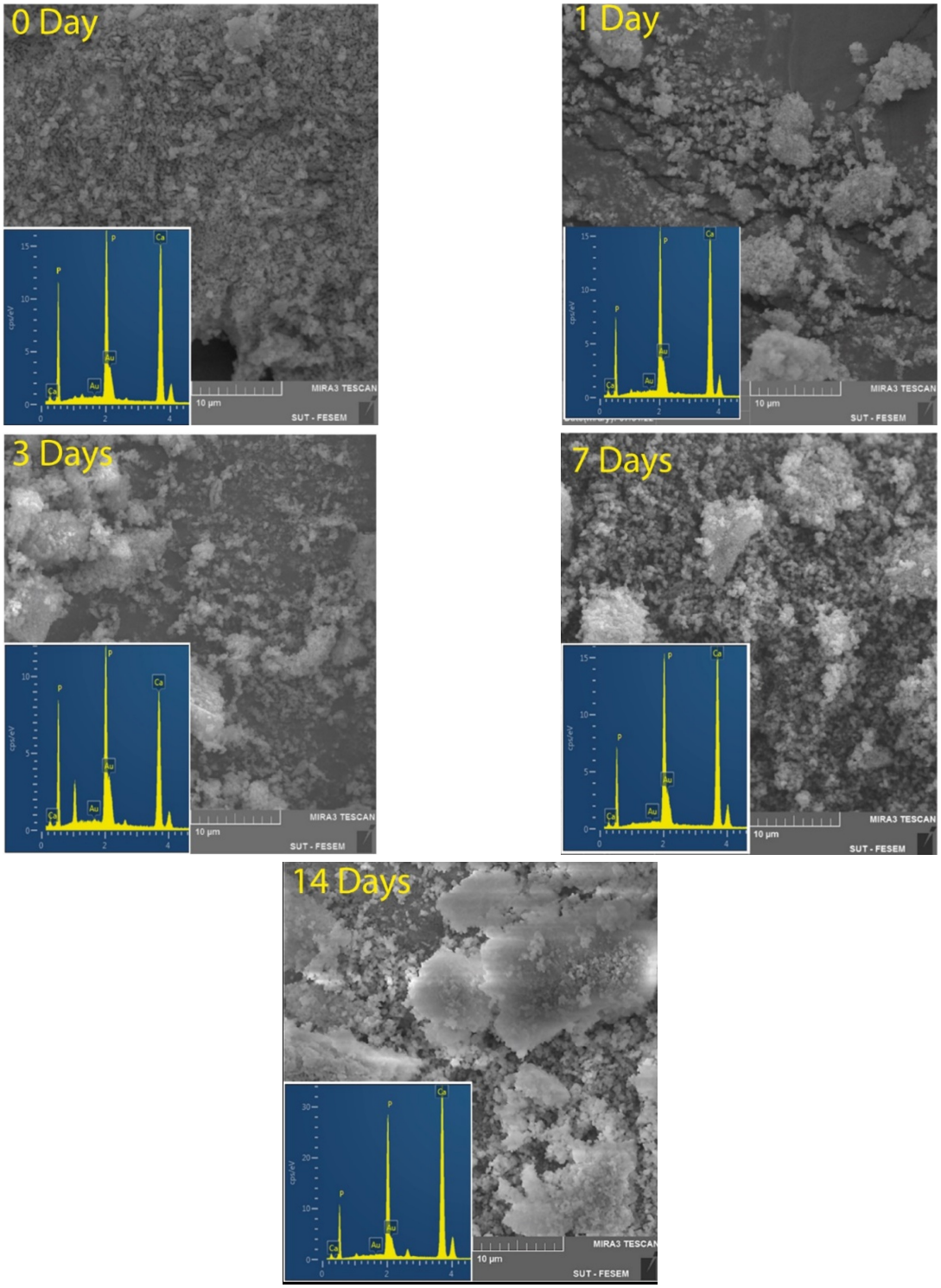

Figure 5. FESEM and EDX images of the HA (FB-900 °C) after immersion in the SBF for 14 days.

After just one day in the SBF, the surface of each sample exhibited evidence of apatite particle development (Figure 5). After a period of one day, increased apatite particle growth was seen. The smaller crystals are to blame for this, given their increased surface area and greater reactivity, which made it possible to significantly and quickly release Ca^{2+} ions [13]. After 7 and 14 days in the immersion medium, homogeneous development was observed. The length of time that the sediment was submerged resulted in an increase in the apatite layer's thickness that had just been produced. The Energy Dispersive X-Ray (EDX) analysis revealed that the majority of the formed surface particles were composed of calcium, phosphorus, and oxygen, demonstrating the formation of calcium of the calcium-phosphorus-rich apatite-layer.

CONCLUSIONS

The HA extracted from carp bones can be an alternative to synthetic HA. HA was found to have an agglomerated, spherical morphology. The crystal structure of the biological HA was a good match with the synthetic HA. The main functional groups were detected in the extracted HA structure. The highest dissolution rate was observed after the first day of immersion in the SBF. The extracted HA was bioactive and had enhanced apatite growth. Overall, the results indicate that the extracted HA from the fish bones have great promise as a biomaterial with several possible uses.

REFERENCES

1. Akram M., Ahmed R., Shakir I., Ibrahim W. A. W., Hussain R. (2014): Extracting hydroxyapatite and its precursors from natural resources. *Journal of Materials Science, 49*, 1461-1475. Doi:10.1007/s10853-013-7864-x
2. Piccirillo C., Pullar R. C., Costa E., Santos-Silva A., Pintado M. M. E., Castro P. M. L. (2015): Hydroxyapatite-based materials of marine origin: A bioactivity and sintering study. *Materials Science and Engineering: C, 51*, 309-315. Doi:10.1016/j.msec.2015.03.020
3. Alshemary A. Z., Akram M., Taha A., Tezcaner A., Evis Z., Hussain R. (2018): Physico-chemical and biological properties of hydroxyapatite extracted from chicken beaks. *Materials Letters, 215*, 169-172. Doi:10.1016/j.matlet.2017.12.076
4. Odusote J. K., Danyuo Y., Baruwa A. D., Azeez A. A. (2019): Synthesis and characterization of hydroxyapatite from bovine bone for production of dental implants. *Journal of Applied Biomaterials & Functional Materials, 17*, 2280800019836829. Doi:10.1177/2280800019836829
5. Dabiri S. M. H., Rezaie A. A., Moghimi M., Rezaie H. (2018): Extraction of hydroxyapatite from fish bones and its application in nickel adsorption. *BioNanoScience, 8*, 823-834. Doi:10.1007/s12668-018-0547-y
6. Muhammad N., Gao Y., Iqbal F., Ahmad P., Ge, R., Nishan U., Rahim A., Gonfa G., Ullah Z. (2016): Extraction of biocompatible hydroxyapatite from fish scales using novel approach of ionic liquid pretreatment. *Separation and Purification Technology, 161*, 129-135. Doi:10.1016/j.seppur.2016.01.047
7. Vijayaraghavan P., Rathi M., Almaary K. S., Alkhattaf F. S., Elbadawi Y. B., Chang S. W., Ravindran B. (2022): Preparation and antibacterial application of hydroxyapatite doped Silver nanoparticles derived from chicken bone. *Journal of King Saud University-Science, 34*, 101749. Doi:10.1016/j.jksus.2021.101749
8. Mustafa N., Ibrahim M. H. I., Asmawi R., Amin A. M. (2015): Hydroxyapatite extracted from waste fish bones and scales via calcination method. *Applied Mechanics and Materials, 773*, 287-290. Doi:10.4028/www.scientific.net/AMM.773-774.287
9. Boutinguiza M., Pou, J., Comesaña R., Lusquiños F., de Carlos, A., León B. (2012): Biological hydroxyapatite obtained from fish bones. *Materials Science and Engineering: C, 32*, 478-486. Doi:10.1016/j.msec.2011.11.021
10. Yamamura H., da Silva V. H. P., Ruiz P. L. M., Ussui V., Lazar D. R. R., Renno A. C. M., Ribeiro D. A. (2018): Physico-chemical characterization and biocompatibility of hydroxyapatite derived from fish waste. *Journal of the Mechanical Behavior of Biomedical Materials, 80*, 137-142. Doi:10.1016/j.jmbbm.2018.01.035
11. Nilen R., Richter P. (2008): The thermal stability of hydroxyapatite in biphasic calcium phosphate ceramics. *Journal of Materials Science: Materials in Medicine, 19,* 1693-1702. Doi:10.1007/s10856-007-3252-x.
12. Sanosh K. P., Chu M.-C., Balakrishnan A., Kim T. N., Cho S.-J. (2010): Sol–gel synthesis of pure nano sized β-tricalcium phosphate crystalline powders. *Current Applied Physics, 10*, 68-71. Doi:10.1016/j.cap.2009.04.014
13. Yousefi A.-M., Oudadesse H., Akbarzadeh R., Wers E., Lucas-Girot A. (2014): Physical and biological characteristics of nanohydroxyapatite and bioactive glasses used for bone tissue engineering. *Nanotechnology Reviews, 3*, 527-552. Doi:10.1515/ntrev-2014-0013